

Journal Pre-proof

Long-term performance of silane coupling agent/metakaolin based geopolymer

Changsen Zhang, Xu Wang, Zhichao Hu, Qisheng Wu, Huajun Zhu, Jinfan Lu



PII: S2352-7102(20)33723-2

DOI: <https://doi.org/10.1016/j.jobe.2020.102091>

Reference: JOBE 102091

To appear in: *Journal of Building Engineering*

Received Date: 26 July 2020

Revised Date: 8 December 2020

Accepted Date: 9 December 2020

Please cite this article as: C. Zhang, X. Wang, Z. Hu, Q. Wu, H. Zhu, J. Lu, Long-term performance of silane coupling agent/metakaolin based geopolymer, *Journal of Building Engineering*, <https://doi.org/10.1016/j.jobe.2020.102091>.

This is a PDF file of an article that has undergone enhancements after acceptance, such as the addition of a cover page and metadata, and formatting for readability, but it is not yet the definitive version of record. This version will undergo additional copyediting, typesetting and review before it is published in its final form, but we are providing this version to give early visibility of the article. Please note that, during the production process, errors may be discovered which could affect the content, and all legal disclaimers that apply to the journal pertain.

© 2020 Published by Elsevier Ltd.

Author statement

Changsen Zhang: Revising-Reviewing, Editing and Supervision. **Xu Wang:** Data curation, Writing-Original draft preparation. **Hu Zhichao:** Investigation. **Qisheng Wu:** Supervision. **Huajun Zhu:** Supervision. **Jinfan Lu:** Documentation support. All authors read and contributed to the manuscript.

Journal Pre-proof

22 the geopolymer is significantly enriched after adding silane coupling agent.

23 **Key words:** metakaolin; silane coupling agent; geopolymer; long term performance

24

25 **1. Introduction**

26 Concrete is one of the most widely used building materials, traditionally
27 produced by using ordinary portland cement (OPC) as major binder. However, the
28 environmental problems caused by the emission of large amounts of carbon dioxide
29 (CO_2) during the production of cement have attracted more and more attention [1-5].
30 The production of 1 ton of cement is accompanied by the production of 0.6 to 1 ton of
31 CO_2 , and it is accompanied by the production of other harmful gases [6, 7]. This
32 promotes the use of geopolymer, a new type of green cementitious material, and
33 readily available raw materials such as metakaolin (MK), fly ash (FA) and ground
34 blast furnace slag powder (GGBS) can be used for preparation. In addition,
35 geopolymer can also reduce CO_2 emissions by 26-45% without losing economic
36 benefits [8, 9]. The excellent properties of geopolymer gradually make it an
37 alternative to OPC [10]. Recently, more researches have shown that the use of
38 alkaline activators can activate cementitious materials, and can directly prepare
39 geopolymer concrete without using OPC [11-13]. The zeolite-like gel (N-A-S-H) with
40 a high degree of polymerization can be produced through the polymerization reaction
41 of the silico-alumina material under alkaline conditions. The basic structure of
42 geopolymer is a three-dimensional network structure with random distribution of
43 $[\text{SiO}_4]^{4-}$ and $[\text{AlO}_4]^{5-}$ tetrahedron, and alkali metals distribute between network pores

44 to balance the electric charge [14].

45 As a new type of green alkali-activated cementitious material, geopolymer has
46 made remarkable progress in many aspects, such as basic theory preparation and
47 application technology, but it has not been widely used in commercial applications.
48 One of the reasons is the lack of long-term basic data support such as durability and
49 product stability [15, 16]. In recent years, in order to prove that alkali-activated
50 cementitious materials can withstand the test of time, many scholars have studied the
51 change of properties, hydration products and microstructure evolution of long-term
52 alkali-activated cementitious materials. Wardhono et al. [17] studied the engineering
53 performance of alkali slag geopolymer (AAS) and low calcium fly ash geopolymer
54 (FAGP) for up to 540 days, and found that the compressive strength, elastic modulus
55 and impermeability of AAS were better than FAGP in the first 90 days. However, it
56 can be seen that the performance of FAGP has been significantly improved and the
57 performance of AAS concrete has declined on the contrary from the results of
58 performance comparison between 90 days and 540 days. In addition, the microscopic
59 morphology of FAGP gradually became dense, while microcracks appeared on the
60 surface of AAS and gradually expanded after 90 days. Tian et al. [18] mixed bagasse
61 fiber and steel fiber with high content fly ash (HVFA) to prepare a green cementitious
62 material, and studied the physical and mechanical properties at the age of 28 days, 3
63 months, 6 months and 10 months. The results show that the compressive strength,
64 Young's modulus, fracture modulus and tensile strength of the composite decrease
65 with the decrease of the content of fly ash and bagasse fiber, but the bending

66 toughness increases with the increase of the content of fly ash. The increased use of
67 fly ash and bagasse fiber both reduced the bulk density of samples and increased the
68 apparent porosity and water absorption. The effect will be more obvious as the curing
69 time is extended. In summary, it is worth to study the long-term maintenance
70 performance of geopolymer, which will affect whether geopolymer can be widely
71 used in actual projects. At present, the toughening of geopolymer is mainly through
72 the addition of fibers and other auxiliary materials, and there are relatively few reports
73 on the use of organic polymers to toughen geopolymer.

74 In this paper, silane coupling agent (KH-550) is selected as the modifier on the
75 basis of related research to explore the long-term durability of silane coupling
76 agent/metakaolin-based geopolymer [19, 20]. The geopolymer samples were cured for
77 up to 28 days, 56 days, 90 days, 180 days and 360 days respectively. The long-term
78 performance of geopolymer were analyzed by X-ray diffraction (XRD), scanning
79 electron microscope (SEM) and other characterization methods to analyze the mineral
80 phase composition and microstructure of modified geopolymer with different curing
81 ages. It is of high research significance to study the influence of organic polymers on
82 the durability of cementitious materials.

83 **2. Materials and methodology**

84 *2.1 Materials*

85 Metakaolin (MK) was purchased from Gongyi Mine Co., Ltd (Henan, China),
86 which is made from high-temperature calcination of kaolin. Quartz (main mineral),
87 Kaolinite and Aluminum Hydroxide were identified in XRD pattern (Fig. 1) of MK.

88 The particle size distribution parameter (D_{50}) of MK in Fig. 2 is 20.33 μm (measured
89 by LS 13320 laser diffraction particle size analyzer). The chemical composition
90 analyses of MK are listed in Table 1. Sodium silicate solution was purchased from the
91 market and was produced by Nanchang Junbang Chemical Co., Ltd (Jiangxi, China).
92 The alkaline activator is prepared by adding sodium hydroxide (purity \geq 96%) and
93 distilled water to the sodium silicate solution (8.54% Na_2O , 27.30% SiO_2). Silane
94 coupling agent (SCA) was purchased from Shandong Yousuo Chemical Technology
95 Co., Ltd. and the characteristics of silane coupling agent are listed in Table 2.

96 *2.2 Preparation of geopolymer samples*

97 It should be noted that the silane coupling agent needs to be hydrolyzed in
98 advance before use. An appropriate amount of silane coupling agent was added to
99 distilled water and stirred at high speed for 20 minutes, and then glacial acetic acid
100 was added to adjust the pH value. The alkali activator was prepared by mixing sodium
101 silicate solution with sodium hydroxide to achieve a 1.5 modulus (molar ratio of SiO_2
102 to Na_2O) and a concentration parameter of 37%. The prepared alkali activator is
103 cooled to room temperature to equilibrate. The mixing composition and ratio of
104 geopolymer paste are shown in Table 3. The Alkali activator was poured into the
105 metakaolin and stirred slowly for 2 minutes, then rapidly stirred for 2 minutes to
106 obtain geopolymer precursor. Different proportions of silane coupling agent after
107 hydrolysis were added to geopolymer precursor and stirred at high speed for 2
108 minutes to obtain geopolymer slurry. Geopolymer slurry was cast into resin molds of
109 20 mm \times 20 mm \times 20 mm (for compressive strength test) and 20 mm \times 20 mm \times 80

110 mm (for flexural strength test). The prepared samples were placed in a curing
111 chamber at room temperature (20°C) and relative humidity > 95% for 24 hours, then
112 demold and cure the hardened sample for 28 days, 56 days, 90 days, 180 days and 360
113 days.

114 *2.3 Mechanical performance test and characterization methods*

115 The compressive strength of specimens was tested by fully automatic
116 compressive bending machine (model WHY-200) and the flexural strength was
117 determined by electronic universal testing machine (model RGM-4010). The mineral
118 composition of samples solidified at different ages was characterized by using X-ray
119 diffraction (model DX-2700) at a scanning rate of 6°/min with CuK α radiation of $2\theta =$
120 5° - 80° . Nicolet Fourier Transform Infrared Spectrometer (STD11202624D) was used
121 to record the spectrum in the 400-4000 cm^{-1} area. The spectra of hybrid geopolymer
122 were recorded at different aging times (28 days, 56 days, 90 days, 180 days and 360
123 days) to study the development of aluminosilicate framework during geological
124 polymerization. The pore structure has a significant effect on the strength and
125 durability of the material. The PoreMaster 60GT automatic mercury porosimeter is
126 used to test the pore structure. Field emission scanning electron microscope (JEOL,
127 model JSM-7001F) was used to observe the microscopic morphology of different
128 specimens.

129 **3. Results and discussion**

130 *3.1 Compressive strength analysis*

131 Fig. 3 shows the compressive strength of samples with different contents of

132 silane coupling agent at different curing ages. As the amount of silane coupling agent
133 increases, the compressive strength of samples first increases and then decreases. It is
134 interesting that when curing reaches 90 days, the compressive strength of specimens
135 doped with silane coupling agent is significantly improved. The compressive strength
136 of the sample doped with 0.1wt% silane coupling agent reached 51.4 MPa at 90 days,
137 which was 14.99% higher than that at 28 days. The increase in compressive strength
138 before 90 days indicates that the silane coupling agent is hydrolyzed to obtain organic
139 functional groups, and the Si-OH bond and Al-OH bond formed in the early
140 geopolymerization process realize the chemical bonding reaction. This also promotes
141 the formation of more geopolymer gels and compacts the structure. With the
142 extension of curing time, the strength of geopolymer specimens began to decline after
143 90 days. The strength of specimens containing 0.1wt% silane coupling agent is 41.7
144 MPa, which is 6.71% lower than that of the 28-day cured samples. The decrease in
145 strength after 90 days may be due to the samples being exposed to the air and being
146 carbonized and harmful ions Invasion.

147 *3.2 Flexural strength analysis*

148 The flexural strength of samples under different curing ages is shown in Fig. 4.
149 As the amount of silane coupling agent increases, the flexural strength of silane
150 coupling agent/metakaolin-based geopolymer samples gradually decreases. This
151 indicates that excessive addition of silane coupling agent has a negative effect on the
152 bending strength of geopolymer. However, with the extension of curing time, the
153 flexural strength of specimens increases first and then decreases. The strength of

154 samples cured for 90 days was significantly improved, and the sample containing 0.1
155 wt% silane coupling agent was the best. The strength of samples mixed with 0.1wt%
156 silane coupling agent reached 12.96 MPa, which was 11.34% higher than curing for
157 28 days. This indicates that the silane coupling agent/metakaolin-based geopolymer is
158 undergoing continuous geopolymerization in the first 90 days. After curing for 90
159 days, the strength of specimens dropped sharply. This is because the polymerization
160 reaction produced an excessive amount of sodium aluminosilicate gel (N-A-S-H),
161 which increased the crack propagation and caused the performance of geopolymer to
162 decrease [21].

163 3.3 XRD analysis

164 According to the above analysis, MS-0.1 has the best performance, so the
165 mineral composition of the samples under different curing cycles was analyzed in
166 combination with XRD patterns (Fig.5). The diffraction peaks of geopolymers are
167 concentrated at about 20-30°, which is attributed to the high content of quartz in
168 geopolymers. The diffraction peak at 12° corresponds to unreacted kaolinite. The
169 amorphous diffraction peaks between 25° and 30° are mainly quartz phase. Therefore,
170 long-term curing and the addition of silane coupling agents have no effect on the
171 crystalline phase of the metakaolin-based geopolymer mineral phase, and the
172 geopolymer mineral phase is still amorphous [22]. The mineral composition of the
173 MS-0.1 sample in the first 90 days is no different, this is because the gel phase
174 generated after polymerization is amorphous. It is strange that the diffraction peak
175 intensity of samples cured for 180 days and 360 days at about 27°~29° decreases with

176 the extension of the curing time. This is due to part of the SiO_2 involved in the
177 polymerization reaction and the diffraction peak intensity at about 25° is the residual
178 quartz phase during the polycondensation process [23, 24].

179 3.4 FT-IR analysis

180 To determine the effect of silane coupling agent in metakaolin based geopolymer
181 and the changes of geopolymer samples under long-term conservation, geopolymer
182 samples of different curing ages were collected and analyzed by FT-IR spectroscopy. ,
183 It can be observed from Fig. 6 that the main vibration modes in the FT-IR spectrum of
184 metakaolin (MK) are SiAOASi asymmetric stretching at 1076 cm^{-1} , SiAOAAI at 810
185 cm^{-1} and SiAO bending at 458 cm^{-1} , this corresponds to the metakaolin formed after
186 calcining kaolin [25]. In the infrared spectrum of metakaolin, the unique SiAOAAI
187 band at 810 cm^{-1} disappeared in geopolymer, indicating that the geopolymerization
188 reaction was complete. The absorption peak at 561 cm^{-1} in the figure corresponds to
189 the bending vibration of AlAOASi, and the absorption peak at 701 cm^{-1} is caused by
190 the symmetrical vibration of the four-coordinate atomic group TO_4 [26, 27]. The
191 bands near 3446 cm^{-1} and 1641 cm^{-1} are caused by OAH stretching and bending
192 vibrations of absorbed water molecules [21]. At the same time, the peak intensity of
193 specimens mixed with 0.1wt% silane coupling agent in this band is significantly
194 higher than that of metakaolin, which further shows that under the action of silane
195 coupling agent and alkali activator, the polymerization reaction occurs and produces
196 more OH groups. However, with the extension of the curing period, the peak intensity
197 weakened, because the sample will react with CO_2 for a long time when it is exposed

198 to the air [28]. The strongest vibration wide band can be observed at 900-1100 cm^{-1} ,
199 which is mainly attributed to the tensile vibration of TAOASi band (T=Si or Al). This
200 is consistent with previous studies [29, 30], and it is possible that C-(A)-S-H and
201 N-A-S-H gels centered on 980 and 1000 cm^{-1} wavenumbers. Interestingly, with the
202 extension of the curing period, the SiAO band shifted to a lower wavenumber, which
203 indicates that SiO_4 is replaced by AlO_4 in the gel of geopolymers and causes the local
204 chemical environment of the Si-O bond to change [31].

205 *3.5 Pore structure analysis*

206 For the purpose of discussing the effect of silane coupling agent on geopolymer
207 samples under long-term curing and the changes in the internal pore structure of
208 geopolymer samples, mercury intrusion tests were carried out on MS-0.1 samples
209 cured for 28d, 90d and 360d. The pore size distribution of the geopolymer sample is
210 shown in Fig. 7. It can be seen that with the extension of curing time, the volume of
211 gel pores ($\leq 10\text{nm}$) in the pore structure increases, and the total volume of pores
212 (10-100 nm) decreases, but the volume of harmful pores ($\geq 50\text{nm}$) is almost no change
213 [32]. The total porosity under the three curing ages are 27.15%, 26.64% and 26.76%
214 respectively. The total porosity at 90 days is the smallest and contains more gel pores,
215 which also corresponds to the optimal performance of geopolymer cured for 90 days.
216 Another interesting finding is that the closest pore size of the sample is reduced from
217 13.16nm to 8.11nm. This indicates that the silane coupling agent participates in the
218 polymerization reaction to generate an enriched N-A-S-H gel, which refines the pore
219 structure of the silane coupling agent/metakaolin based geopolymer [32]. However,

220 the most probable pore size increased to 10.83 nm at 360 days and the total porosity
221 also increased, which was caused by crack propagation [17].

222 *3.6 SEM analysis*

223 The geopolymer specimens cured for 28 days, 90 days and 360 days were
224 analyzed by SEM to observe the internal structure changes of MS-0.1 under long-term
225 curing. In Fig. 8(a), unreacted metakaolin particles and aluminosilicate gel matrix
226 (N-A-S-H) are observed. Unreacted or partially reacted metakaolin particles appear in
227 the form of composite materials, which have a significant impact on the overall
228 strength of the geopolymer material [33]. In addition, it can be found that needle-like
229 material (KH550) is attached to the geopolymer with fewer cracks and pores. This
230 shows that the addition of silane coupling agent can promote the dense structure of
231 geopolymer. The interesting finding is that the needle-like substance disappeared after
232 90 days of curing, and the gel content in samples increased significantly. The
233 enrichment of gel and the continuous cladding make the structure of the geopolymer
234 compact [32]. This is strong evidence explaining the high-strength geopolymer
235 samples cured for 90 days. However, increased crack propagation and crack depth
236 appear in Fig. 8(c), which is the microscopic morphology of the sample after 360 days
237 of curing. On the one hand, it is due to the combined effect of pressure separation and
238 self-drying, on the other hand, it is caused by excess gel [17].

239 **4. Conclusions**

240 Silane coupling agent was added to metakaolin based geopolymer, and the
241 mechanical properties and microstructure changes of specimens cured for 360 days

242 were observed and discussed. The compressive strength and flexural strength of the
243 long-term cured samples have increased during the first 90 days, while the strength
244 gradually decreased during 90-360 days. The compressive strength and bending
245 strength of the geopolymer sample with a silane coupling agent content of 0.1wt% at
246 90 days were 51.4 MPa and 12.93 MPa, respectively. Compared with the samples
247 cured for 28 days, they were increased by 14.99% and 11.24% respectively. The
248 addition of silane coupling agent does not change the mineral phase composition of
249 the geopolymer, but the addition of silane coupling agent enriches the gel phase in
250 geopolymer.

251

252 **Acknowledgements**

253 Acknowledged financial supports include the National Natural Science
254 Foundation of China (51672236, 51502259 and 51572234).

255

256

257 **References**

- 258 [1] C. Meyer, The greening of the concrete industry, *Cem. Concr. Compos.* 31 (2009)
259 601-605.
- 260 [2] A. Bosoaga, O. Masek, J.E. Oakey, CO₂ Capture Technologies for Cement
261 Industry, *Energ Proc.* 1 (2009) 133-140.
- 262 [3] C. Chen, G. Habert, Y. Bouzidi, A. Jullien, Environmental impact of cement
263 production: detail of the different processes and cement plant variability
264 evaluation, *J. Clean. Prod.* 18 (2010) 478-485.

- 265 [4] J. Chen, L. Shen, Q. Shi, J. Hong, J.J. Ochoa, The effect of production structure
266 on the total CO₂ emissions intensity in the Chinese construction industry, J.
267 Clean. Prod. 213 (2019) 1087-1095.
- 268 [5] T.M. Letcher. Why do we have global warming, *Manag. Global. Warm.* 1 (2019)
269 3-15.
- 270 [6] C. Li, X.Z. Gong, S.P. Cui, Z.H. Wang, CO₂ emissions due to cement
271 manufacture, *Mater. Sci. Forum.* 685 (2011) 181-187.
- 272 [7] J. Peng, L. Huang, Y. Zhao, P. Chen, L. Zeng, W, Zheng, Modeling of carbon
273 dioxide measurement on cement plants, *Adv. Mater. Res.* 610-613 (2013)
274 2120-2128.
- 275 [8] B.C. McLellan, R.P. Williams, J. Lay, A.V. Riessen, G.D. Corder, Costs and
276 carbon emissions for geopolymer pastes in comparison to ordinary portland
277 cement, *J. Clean Prod.* 19 (2011) 1080-1090.
- 278 [9] G. Habert, J.B. d'Espinose de Lacaillerie, N. Roussel, An environmental
279 evaluation of geopolymer based concrete production: reviewing current research
280 trends, *J. Clean. Prod.* 19 (2011) 1229-1238.
- 281 [10] Z. Zhang, Y. Zhu, T. Yang, L. Li, H. Zhu, H. Wang, Conversion of local
282 industrial wastes into greener cement through geopolymer technology: A case
283 study of high-magnesium nickel slag, *J. Clean. Prod.* 141 (2017) 463-471.
- 284 [11] W.D.A. Rickard, G.J.G. Gluth, K. Pistol, In-situ thermo-mechanical testing of fly
285 ash geopolymer concretes made with quartz and expanded clay aggregates, *Cem.*
286 *Concr. Res.* 80 (2016) 33-43.
- 287 [12] B. Singh, Ishwarya. G, M. Gupta, S.K. Bhattacharyya, Geopolymer concrete: a
288 review of some recent developments, *Constr. Build. Mater.* 85 (2015) 78-90.

- 289 [13] M. Soutsos, A.P. Boyle, R. Vinai, A. Hadjierakleous, S.J. Barnett, Factors
290 influencing the compressive strength of fly ash based geopolymers, *Constr. Build.*
291 *Mater.* 110 (2016) 355-368.
- 292 [14] J.W. Phair, J.S.J. Van Deventer, Characterization of fly-ash-based geopolymeric
293 binders activated with sodium aluminate. *Ind. Eng. Chem. Res.* 41 (2002)
294 4242-4251.
- 295 [15] O. F. Nnaemeka, N.B. Singh. Durability properties of geopolymer concrete made
296 from fly ash in presence of Kaolin, *Mater. Today. Proc.* In Press.
- 297 [16] J.L. Provis, Alkali-activated materials, *Cem. Concr. Res.* 114 (2018) 40-48.
- 298 [17] A. Wardhono, C. Gunasekara, D.W. Law, S. Setunge. Comparison of long term
299 performance between alkali activated slag and fly ash geopolymer concretes,
300 *Constr. Build. Mater.* 143 (2017) 272-279.
- 301 [18] H. Tian, Y.X. Zhang, The influence of bagasse fibre and fly ash on the long-term
302 properties of green cementitious composites, *Constr. Build. Mater.* 111 (2016)
303 237-250.
- 304 [19] C. Zhang, B. Zhu, Q. Wu, Y. Li, Z. Feng, Y. Wang, Z. Hu. Physical properties and
305 microstructure of nickel slag/metakaolin based geopolymer with different
306 contents of nickel slag, *Adv. Cem. Res.* 32 (2018) 1-31.
- 307 [20] C. Zhang, Z. Hu, H. Zhu, X. Wang, J. Gao. Effects of silane on reaction process
308 and microstructure of metakaolin-based geopolymer composites, *J. Build. Eng.*
309 In Press.
- 310 [21] X. Gao, Q.L. Yu, H.J.H. Brouwers, Reaction kinetics, gel character and strength

- 311 of ambient temperature cured alkali activated slag–fly ash blends. *Constr. Build.*
312 *Mater.* 80 (2015) 105-115.
- 313 [22] X. Chen, G.R. Zhu, J. Wang, Q. Chen, Effect of polyacrylic resin on mechanical
314 properties of granulated blast furnace slag based geopolymer, *J. Non-Cryst.*
315 *Solids.* 481 (2018) 4-9.
- 316 [23] P. He, J. Cui, M. Wang, S. Fu, H. Yang, C. Sun, X. Duan, Z. Yang, D. Jia, Y.
317 Zhou, Interplay between storage temperature, medium and leaching kinetics of
318 hazardous wastes in Metakaolin-based geopolymer, *J. Hazard. Mater.* 384 (2020)
319 121377.
- 320 [24] S. Fu, P. He, M. Wang, J. Cui, M. Wang, X. Duan, Z. Yang, D. Jia, Y. Zhou,
321 Hydrothermal synthesis of pollucite from metakaolin-based geopolymer for
322 hazardous wastes storage, *J. Clean. Prod.* 248 (2020) 119240.
- 323 [25] L. Gao, Y. Zheng, Y. Tang, J. Yu, X. Yu, B. Liu, Effect of phosphoric acid content
324 on the microstructure and compressive strength of phosphoric acid-based
325 metakaolin geopolymers, *Heliyon.* 6 (2020) e03853.
- 326 [26] C. Ferone, G. Roviello, F. Colangelo, R. Cioffifi, O. Tarallo, Novel hybrid
327 organic-geopolymer materials, *Appl. Clay. Sci.* 73 (2013) 42-50.
- 328 [27] G. Roviello, L. Ricciotti, C. Ferone, F. Colangelo, O. Tarallo, Fire resistant
329 melamine based organic-geopolymer hybrid composites, *Cem. Concr. Compos.*
330 59 (2015) 89-99.
- 331 [28] M. Catauro, F. Papale, G. Lamanna, F. Bollino, Geopolymer/PEG Hybrid
332 Materials Synthesis and Investigation of the Polymer Influence on Microstructure

- 333 and Mechanical Behavior, *Mater. Res.* 18 (2015) 698-705.
- 334 [29] T.A. Aiken, J. Kwasny, W. Sha, M.N. Soutsos, Effect of slag content and
335 activator dosage on the resistance of fly ash geopolymer binders to sulfuric acid
336 attack, *Cem. Concr. Res.* 111 (2018) 23-40.
- 337 [30] G. Lodeiro, A. F. Jiménez, M.T. Blanco, A. Palomo, FTIR study of the sol-gel
338 synthesis of cementitious gels: C-S-H and N-A-S-H, *J. Sol-Gel. Sci. Technol.* 45
339 (2008) 63-72.
- 340 [31] J. Payne, J. Gautron, J. Doudeau, E. Joussein, S. Rossignol, Influence of calcium
341 addition on calcined brick clay based geopolymers: A thermal and FTIR
342 spectroscopy study, *Constr. Build. Mater.* 152 (2017) 794-803.
- 343 [32] G. Liang, H. Zhu, Z. Zhang, Q. Wu. Effect of rice husk ash addition on the
344 compressive strength and thermal stability of metakaolin based geopolymer,
345 *Constr. Build. Mater.* 222 (2019) 872-881.
- 346 [33] M. Steveson, K. Sagoe-Crentsil, Relationships between composition, structure
347 and strength of inorganic polymers, *J. Mater. Sci.* 40 (2005) 4247-4259.

Table 1. Chemical compositions of metakaolin (MK).

	SiO ₂	Al ₂ O ₃	CaO	MgO	Fe ₂ O ₃	K ₂ O	TiO ₂	Na ₂ O	LOI
MK	48.34	41.05	2.43	-	4.44	0.31	3.44	-	0.62

Table 2. Characteristics of silane coupling agent (SCA).

SCA	Chemical formula	Molecular weight, (g/mol)	Water miscibility	Stability in pore solution
KH-550	$\text{NH}_2(\text{CH}_2)_3\text{Si}(\text{OC}_2\text{H}_5)_3$	221.37	Totally soluble	Stable for 24 h

Table 3. The composition percentage of the alkali activator (% by weight).

	Sodium hydroxide	Sodium silicate solution	Distilled water (additional)
Alkaline activator	12.108	87.892	6.6

Table 4. Mixtures proportions of geopolymer pastes.

Samples	MK contents (g)	Alkaline activator (g)	Silane coupling agent (KH-550) (g)
MS-0	330	231	0
MS-0.1	330	231	0.33
MS-0.2	330	231	0.66
MS-0.5	330	231	1.65
MS-1	330	231	3.3

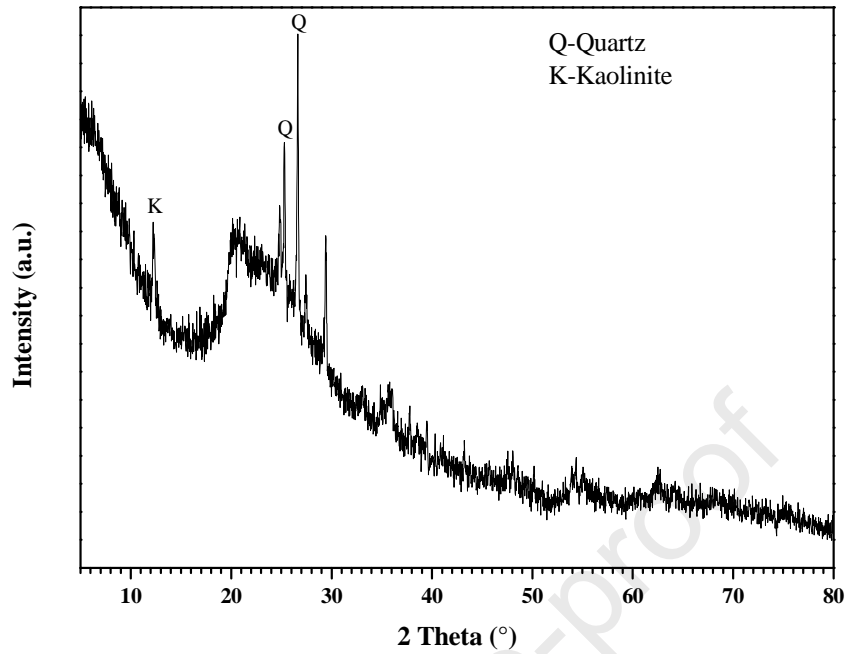


Fig.1. XRD pattern of metakaolin (MK).

Phases identified: Kaolinite, $\text{Al}_2\text{Si}_2\text{O}_5(\text{OH})_4$, PDF No. 14-0164; Quartz, SiO_2 , PDF No. 46-1045

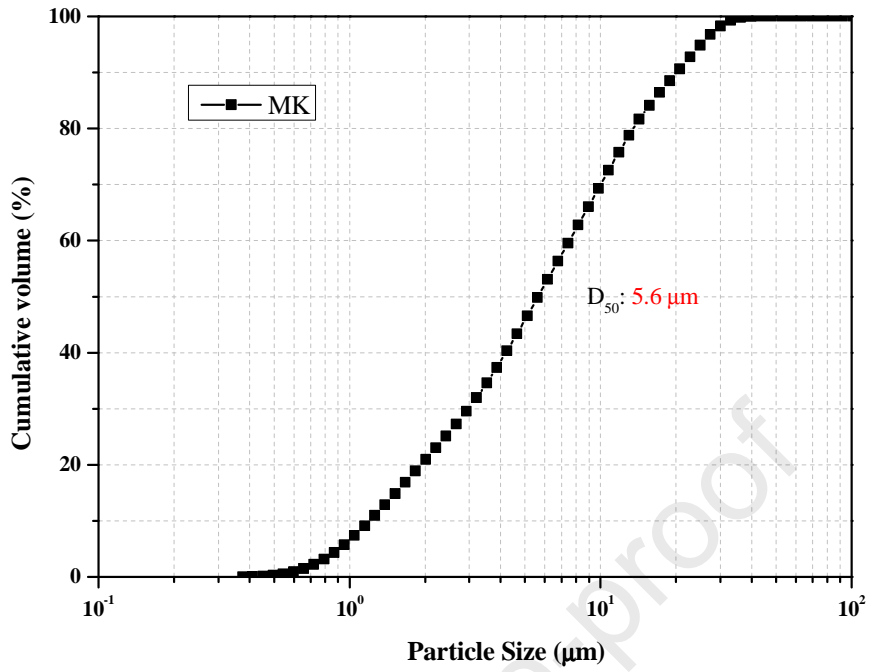


Fig.2. Particle size distribution of metakaolin (MK).

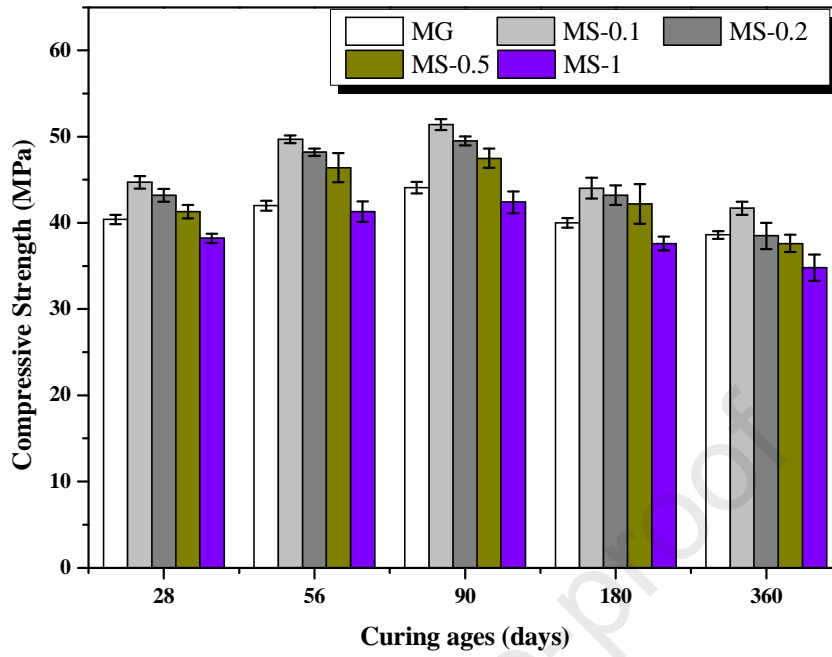


Fig.3. Compressive strength of specimens doped with silane coupling agent at different curing ages.

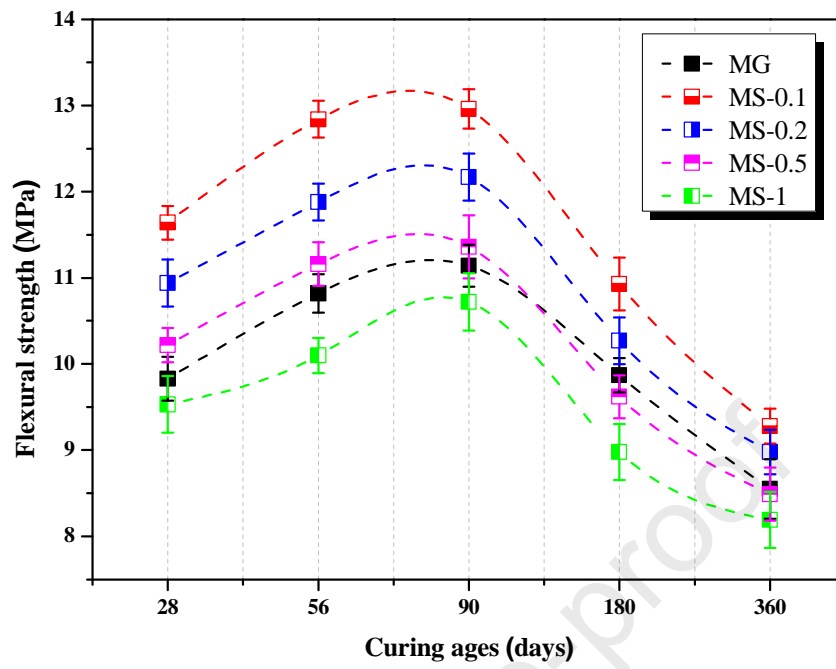


Fig.4. Flexural strength of specimens with different contents of silane coupling agent at different curing ages.

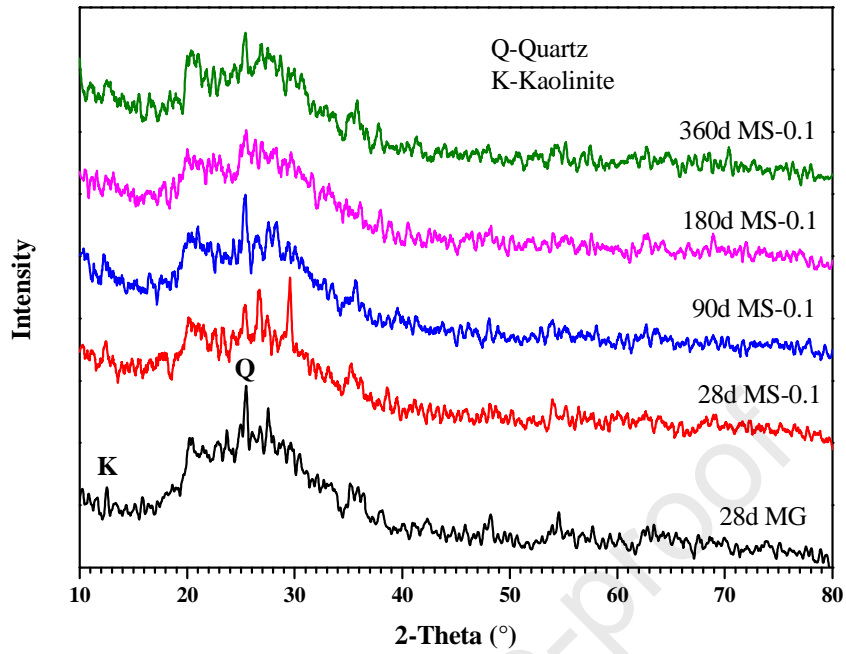


Fig.5. XRD patterns of geopolymer samples cured for different ages.

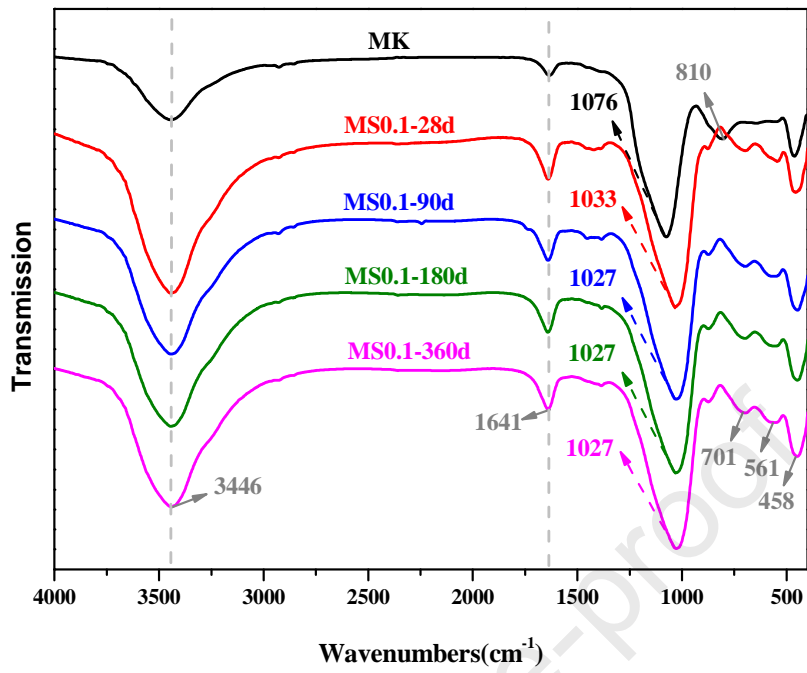


Fig.6. FT-IR images of MK and specimens with 0.1 wt% silane coupling agent cured for up to 360 days.

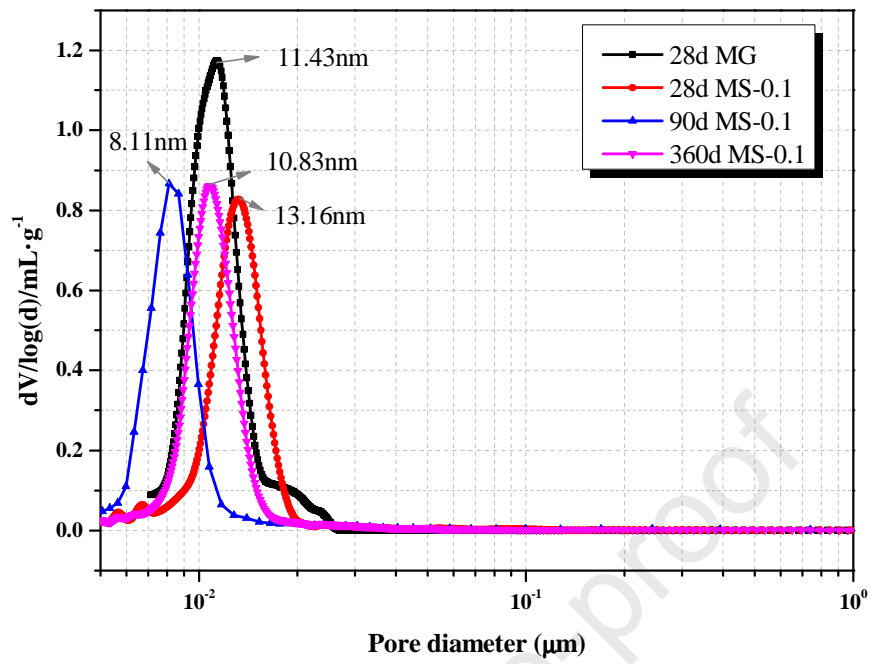


Fig.7. Pore size distribution of MG and MS-0.1 cured for 28 days, 90 days and 360 days.

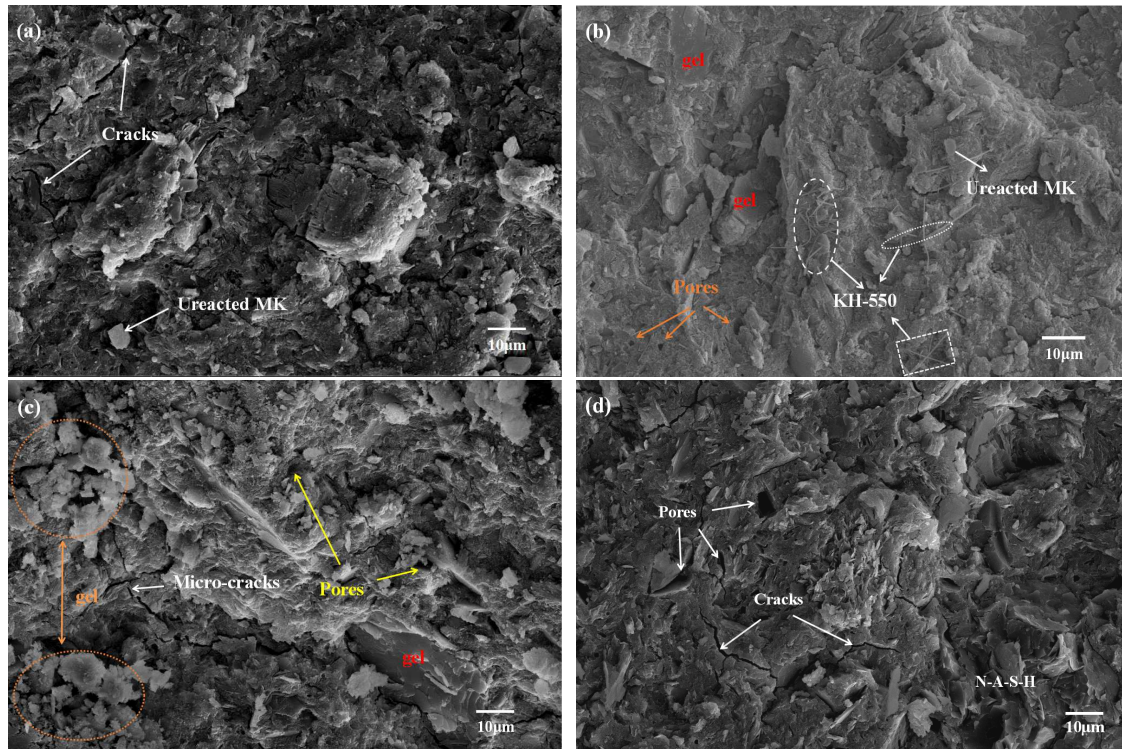


Fig. 8. SEM images of geopolymer samples under different curing ages: (a)MG-28d, (b)MS-0.1-28d, (c) MS-0.1-90d and (d) MS-0.1-360d.

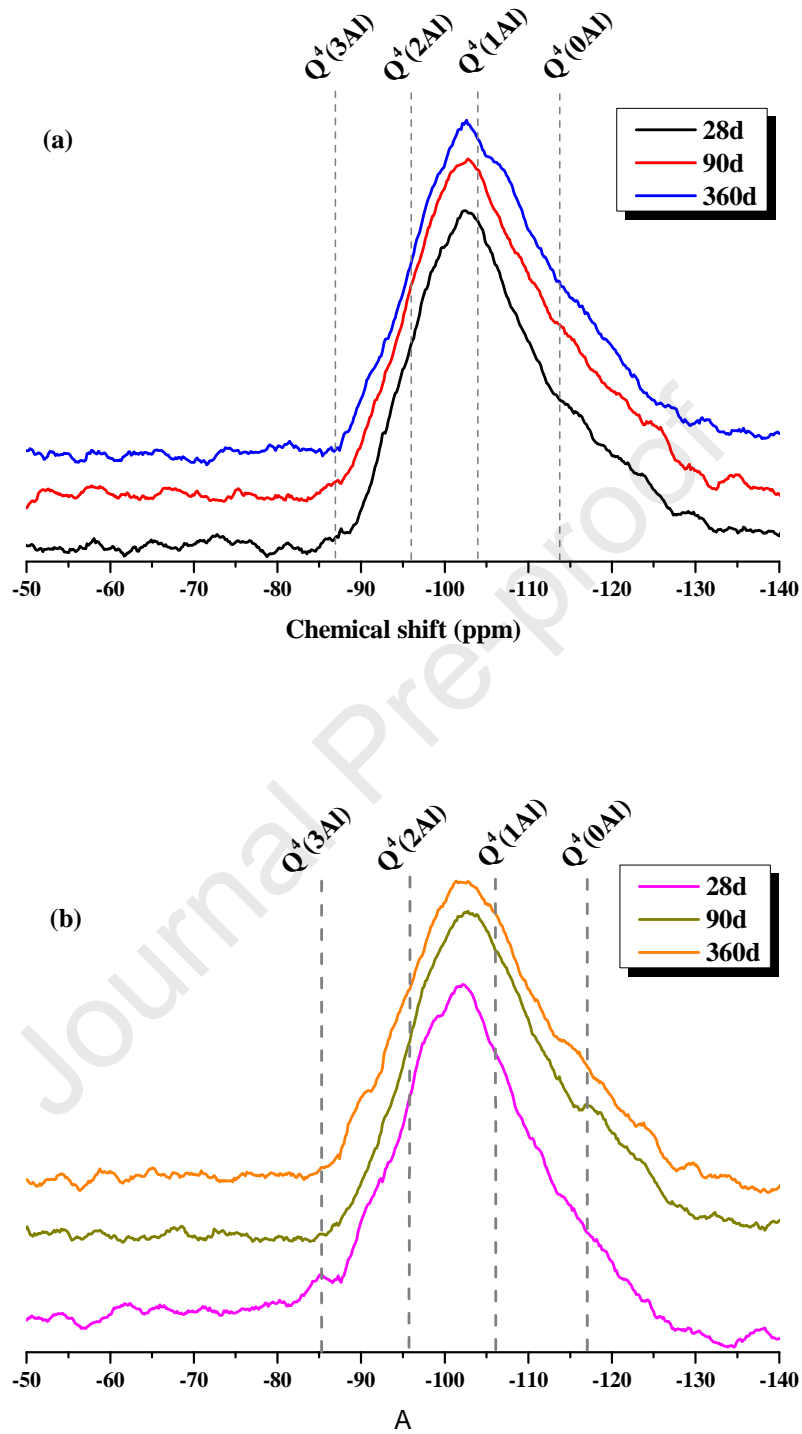


Fig. 9. ^{29}Si NMR analysis of geopolymer samples under different curing ages: (a)MG, (b)MS-0.1.

- Silane coupling agent/metakaolin based geopolymer composites were prepared and conserved for up to 360 days.
- The specimens that cured for 90 days, with the silane coupling agent content of 0.1 wt% showed the best performance.
- Expanded cracks will appear due to the excessive gels and self-desiccation effect in the long term curing.

Journal Pre-proof

Declaration of Interest Statement

No conflict of interest exists in the submission of this manuscript.

Journal Pre-proof